Published in final edited form as:
Circ Cardiovasc Imaging. 2013 November ; 6(6): . doi:10.1161/CIRCIMAGING.113.000674.

MRI Investigation of Macrophages in Acute Cardiac Allograft Rejection after Heart Transplantation

Yijen L. Wu, PhD[1], **Qing Ye, MD**[1], **Danielle F. Eytan, BS**[1], **Li Liu, PhD**[1], **Bedda L. Rosario, PhD**[3], **T. Kevin Hitchens, PhD**[1], **Fang-Cheng Yeh, MD**[1,2], **Nico van Rooijen, PhD**[4], and **Chien Ho, PhD**[1]

[1]Pittsburgh NMR Center for Biomedical Research, and the Department of Biological Sciences, Carnegie Mellon University, Pittsburgh, Pennsylvania [2]Department of Biomedical Engineering, Carnegie Mellon University, Pittsburgh, Pennsylvania [3]Department of Epidemiology, University of Pittsburgh [4]Department of Molecular Cell Biology, VUMC, Amsterdam, The Netherlands

Abstract

Background—Current immunosuppressive therapy after heart transplantation either generally suppresses the recipient's entire immune system or is mainly targeting T-lymphocytes. Monocytes/macrophages are recognized as a hallmark of acute allograft rejection, but the roles that they play are not well characterized *in vivo*, because the tools for accessing *in-situ* macrophage infiltration are lacking. In this study, we utilize MRI to investigate the role of macrophages in acute heart allograft rejection by cellular and functional MRI with selectively depleted systemic macrophages without affecting other leukocyte population and to explore the possibility that macrophages could be an alternative therapeutic target.

Methods and Results—A rodent heterotopic working heart-lung transplantation model was employed for studying acute allograft rejection. Systemic macrophages were selectively depleted by treating recipient animals with clodronate-liposomes. Macrophage infiltration in the graft hearts was monitored by cellular MRI with *in-vivo* ultra-small iron-oxide particles (USPIO) labeling. Graft heart function was evaluated by tagging MRI, followed by strain analysis. Clodronate-liposome-treatment depletes circulating monocytes/macrophages in transplant recipients, and both cellular MRI and pathological examinations indicate a significant reduction in macrophage accumulation in the rejecting allograft hearts. In clodronate-liposome-treated group, allograft hearts exhibit preserved tissue integrity, partially reverse functional deterioration, and prolong graft survival, compared to untreated controls.

Conclusions—Cardiac cellular and functional MRI is a powerful tool to explore the roles of targeted immune cells *in vivo*. Our results indicate that macrophages are essential in acute cardiac allograft rejection, and selective depletion of macrophages with clodronate-liposomes protects hearts against allograft rejection, suggesting a potential therapeutic avenue. Our findings show that there is a finite risk of forming an intra-ventricular mass, presumably from the cellular debris and/or lipid material. Further optimization of the dosing protocol is necessary prior to clinical applications.

Correspondence to: Chien Ho, PhD, Department of Biological Sciences, Carnegie Mellon University, 4400 Fifth Ave, Pittsburgh, PA 15213, Telephone: (412) 268-3395, Fax: (412) 268-7083, chienho@andrew.cmu.edu.
*Dr. Eytan's current institutional affiliation is Cleveland Clinic Lerner College of Medicine of Case Western Reserve University, Cleveland, OH.
YLW, QY, and DFE contributed equally.

Disclosures
None.

Keywords

clodronate-liposomes; cardiac rejection; transplantation; macrophage; magnetic resonance imaging

Macrophage infiltration has long been recognized as a hallmark of acute allograft rejection after heart transplantation; however, the discrete roles of macrophages during the onset and evolution of rejection are not fully understood[1]. Recent reports on various inflammation processes, such as myocardial infarction, cancer, and renal allograft rejection, have revealed that macrophages can play complicated and even conflicting roles. Macrophages have been shown to both increase tissue injury and promote tissue repair, depending on the macrophage phenotype and timing of recruitment [2–4].

To better understand the role of macrophages in rejection, it is necessary to longitudinally and concurrently monitor the macrophage infiltration and graft function as rejection evolves, to examine if they contribute solely in a harmful way, are involved in repairing and functional preservation, or just "innocent bystanders" [1] without playing any critical role. Non-invasive clinical tools for assessing *in-situ* macrophage infiltration on the rejecting sites are lacking. The goal of this study is to investigate whether macrophages play a key role in acute cardiac allograft rejection, using serial non-invasive assessment with cellular and functional MRI.

We have previously shown that cardiac allograft rejection can be detected and graded *in vivo* with both cellular and functional cardiac MRI[5, 6]. *In-situ* macrophage infiltration in rejecting grafts can be evaluated non-invasively and longitudinally over time by labeling monocytes/macrophages in circulation with contrast agents, such as ultra-small iron-oxide (USPIO) particles. USPIO-labeled macrophages are observed by T_2*-weighted MRI and the amount detected is associated with the degree of rejection[5, 6]. We have also demonstrated that cardiac MRI, particularly tagging followed by strain analysis, provides a sensitive measure for evaluating the functional loss as a result of acute allograft rejection. Furthermore, the regions with high macrophage infiltration correlates well with functional impairment [6].

In this study, we used a rodent heterotopic cardiac transplantation model [6] and used liposome-encapsulated-clodronate to selectively deplete circulating monocytes/macrophages [7, 8]. This model allowed us to study the progression of cardiac rejection from early onset to the most severe case, with complete loss of graft function. This study had two objectives: first, to examine whether eliminating monocytes/macrophages in circulation can reduce macrophage populations found in the rejecting graft; and second, to investigate how reducing macrophage populations affect the progression or severity of rejection and loss of cardiac function.

Methods

Animals

All animals used in this study were male inbred Brown Norway (BN; $RT1^n$) and Dark Agouti (DA; $RT1^a$) rats obtained from Harlan (Indianapolis, IN) with a body weight around 250 g. Animal protocols were approved by the Institutional Animal Care and Use Committee of Carnegie Mellon University. All animals received humane care in compliance with the *Guide for the Care and Use of Laboratory Animals*, published by the NIH.

Animal model

This study employed a rodent heterotopic working heart-lung transplantation model in the abdomen, which is described in detail elsewhere[6]. DA-to-BN allograft transplantation results in Grade I rejection on post-operational day (POD) 3–4, Grade II rejection on POD 4–5, Grade III rejection on PODs 5–6, and all grafts are severely rejected (Grade IV) by POD 7. Many allograft hearts stop beating on POD 7, and none can survive past POD 8 without intervention.

DA-to-BN allografts were assigned to one of 3 groups: receiving clodronate-liposome treatment (n = 17); receiving PBS-liposome treatment (n = 11); or allografts receiving no treatment (n = 10). Additionally, BN-to-BN transplantation (n = 4) served as isograft controls. Clodronate-liposomes and control PBS-liposomes were obtained from *clodronateliposomes.org* and their preparation are described elsewhere [8]. Both were administered as a bolus of 1-mL liposome suspension via tail vein on PODs 1, 3, 6, and 8 after transplant surgery. This resulted in a clodronate dose of 28 mg/kg.

At the end-point of the study, ranging from PODs 7–9, organs were harvested and fixed in 4% paraformaldehyde for 24 hrs, followed by storage in PBS at 4 °C.

In-vivo labeling of macrophages with USPIO nanoparticles

Dextran-coated USPIO nanoparticles were used to label macrophages *in vivo* for cellular MRI. The USPIO particles used were either synthesized in our laboratory[9] or purchased from BioPAL, Worchester, MA (Molday ION). Molday ION purchased from BioPAL (http://www.biopal.com/molday-ion.htm) and the USPIO nanoparticles synthesized in our laboratory[9] are both dextran-coated iron-oxide particles, and exhibit similar biophysical and magnetic properties, such as hydrodynamic diameter, zeta potential and relaxivity.

Each animal was given USPIO (4.5 mg iron/kg body weight) intravenously as bolus via tail vein about 20–24 hr prior to the first MRI session on POD 4, and was imaged daily up to POD 9. The blood half-life of USPIO particles in rodents is about 2 hr [10]. Each animal was given sufficient time for (≥ 5 USPIO blood half-life) to allow the USPIO-particles to be cleared before MRI sessions, thus, labeling efficiency and levels should be similar among different animals.

Flow cytometry

Flow cytometry was used to determine the percentage of monocytes/macrophages, lymphocytes, and NK cells in peripheral blood (FACSVantage, Becton Dickinson, Franklin Lakes, NJ). Blood samples were taken from untreated allo-transplant rats (n = 6), PBS-liposome treated allo-transplant rats (n = 5), and clodronate-liposome treated allo-transplant rats (n = 6) prior to sacrifice. The following antibodies and reagents were purchased from AbD Serotec (Oxford, UK): ED1, anti-rat CD68:AlexaFluor488 antibody labels monocytes and macrophages; W3/25:FITC/Ox-8:RPE, anti-rat CD4/CD8; Ox-6, anti-rat major histocompatibility complex class II, RT1.B:FITC (H2A-like) molecule; and BUF09. Ox-39, anti-rat CD25:PE was purchased from eBioscience (San Diego, CA). Data were processed with the FlowJo software (Tree Star, Inc, Ashland, OR).

MRI

In-vivo MRI was performed on a Bruker BioSpec AVANCE III 7-T/21-cm system equipped with a BGA12s gradient set and a 72-mm birdcage RF coil (Bruker Biospin Billerica, MA). Rats were incubated and ventilated as described previously [5, 6]. Core temperature was maintained at 36.8 ± 0.5 °C with a gating and monitoring system (SA Instruments, Stony

Brook, NY). ECG leads were placed on the abdomen to detect the waveform of the transplanted heart.

T_2^*-weighted images were acquired with a FLASH sequence, and tagging was achieved using SPAMM [11, 12]. Nine short-axis slices were used to cover the entire volume of the heart for T_2*-weighted imaging, and a single short-axis slice at mid-ventricular level was used for tagging. Both ECG and respiration triggers were used for gated imaging. The R-wave of ECG was used for cardiac MR trigger. The multiple slices of images were acquired within a repetition time (TR), which was set to be equal to a cardiac cycle, about 180 – 200 ms. Although TR was set to be the cardiac cycle, with respiration gating (60 bpm), the effective TR for MR image acquisition was 1 s. Images were acquired with the following parameters: repetition time= respiration cycle (~1 s); echo time (TE) = 2.7 ms for tagging MRI, and 5 to 7 ms for T_2*-weighted imaging; flip angle (FA) = 30° for T_2*-weighted imaging and 15° for tagging; field of view (FOV) = 4 cm, slice-thickness 1.2 to 1.5 mm, with 156 μm in-plane resolution.

Graft hearts were harvested at the end-point of the study and fixed in 4% paraformaldehyde. Fixed hearts were imaged using a Bruker AVANCE DRX 11.7-T system with a Micro2.5 gradient insert. High-resolution 3D MRM images were acquired with a TR/TE = 480/5.5 ms, and a 46–49 μm isotropic resolution.

Strain and wall-motion analysis

Strains are values that quantify the extent of ventricular deformation throughout cardiac phases: stretching/elongation or compression/shortening. Strains are categorized into two main classes in relation to the heart axes: normal strains are defined in relation to the short-axis planes, and principal strains are defined in relation to the direction of the myocardial fiber bundles. There are three types of strain-tensor sets for each class. Two of the three orthogonal strain-tensor sets, circumferential shortening (Ecc) and radial strain (Err), are presented in this study. HARP (Diagnosoft, Inc. Morrisville, NC) was used for the tagged MRI strain analysis [13, 14]. DICOM images of the tagged MRI time series were read in HARP software, Fourier transformed, then analyzed by the HARP method[13, 14].

3D MR Microscopy (MRM) rendering and visualization

The hypointensity voxels were identified from the 3D volume stack using a signal intensity threshold calculated automatically by Otsu's method [15], which maximized the variance between the hyper- and hypo-intensity voxels. The hypotensity voxels were then represented by the red color. Movie files showing each of the 3D volume rendering sets orbiting through the central axis for better unbiased visualization are shown in Supplemental Figure 1.

Pathological analysis and rejection grade evaluation

Histopathology was performed by the Transplantation Pathology Laboratory of the University of Pittsburgh Medical Center. Graft tissues were subjected to hematoxylin and eosin (H&E) staining and immunohistochemical staining with the mouse anti-rat macrophage antibody ED1 (AbD Serotec) for detecting macrophages and anti-rat T-cell antibody CD3 for detecting T-cells. Rejection grade of the grafts was determined histopathologically according to the International Society for Heart and Lung Transplantation (ISHLT) criteria [16].

Statistical Analysis

Descriptive statistics for leukocytes data were presented as median and interquartile range. Examination of normal distribution assumption for leukocytes data was determined by q-q plots, histograms and Shapiro-Wilk test. For non-normal distributed data, a Kruskal-Wallis

test was performed to test an overall hypothesis of any difference between the three groups (i.e., PBS-liposome, clodronate-liposome and no-treatment) for each leukocyte at POD 7. Adjustment for multiple hypotheses testing (six hypotheses) was performed using the Holm's method. If the overall test was significant, post-hoc comparisons were performed using the Mann-Whitney test and adjustment for multiple comparisons was performed using the Dunn-Sidak adjustment method [17]. Adjusted p-values for multiple hypotheses testing and for post-hoc comparisons were presented. For the strain data, linear mixed-effects models were used to test the main effects of time (POD 5, POD 6, POD 7, POD 8 and POD 9) and group (PBS-liposome, clodronate-liposome, and no-treatment), and time by group interactions on Ecc and Err separately, and to account for within subject correlation. One between-subjects factor (group) and one within-subjects factor (time) and their interaction were defined as fixed effects, and the subject as random effect. After inspecting the correlation within subjects and the autoregressive structure for Ecc, a compound symmetry structure for Err was assumed. The least significant difference method was used for post-hoc comparisons using the Sidak adjustment method. Adjusted p-values for post-hoc comparisons were presented. All statistical analyses were two-sided, and the significance value was $p<0.05$. All analyses were conducted using SAS, version 9.3 statistical software (SAS Institute Inc., Cary, NC). Supplemental Tables 1 and 2 summarize our statistical data.

Results

Clodronate-liposome-treatment selectively depleted monocytes/macrophages

After clodronate-liposome treatment, ED1+ monocytes/macrophages are reduced by more than 90% in blood circulation (Figure 1). A quantitative comparison on POD 7 shows significant differences in ED1+ cells among the groups ($p = 0.039$). Post-hoc comparisons revealed significant smaller ED1+ monocytes/macrophages cells for the clodronate-liposome treatment group when compared to other groups. There was no statistically significant reduction in other leukocyte populations in the blood analyzed by flow cytometry, including CD4+, CD8+, and CD25+ T-lymphocytes, CD161+ [Natural killer (NK)] cells, and RT1B+ B-cells. PBS-liposome treatment does not result in any significant changes in any of the cell types mentioned above. Clodronate-liposome treatment is selective and effectives for depleting macrophages.

Fewer macrophages found in treated allografts

After labeling macrophages with USPIO particles, *in-vivo* T_2*-weighted images of an untreated transplant recipient (Figure 2B) and PBS-liposome treated allograft heart (Figure 2D) show regions of hypointensity in the rejecting allograft heart, indicating the accumulation of USPIO-labeled macrophages. Consistent with diminishing the macrophage infiltration into the graft heart, the clodronate-treated allograft heart (Figure 2C) displays little or no areas of hypointensity.

Figure 3 shows slices from 3D T_2*-weighted MRM of excised hearts (Figure 3 upper panels) and the 3D volume renderings (Figure 3, lower panels) of untreated (Figure 3A, G), clodronate-liposome-treated (Figure 3C, I), and PBS-liposome-treated (Figure 3E, K) allograft hearts. Both untreated and PBS-liposome-treated groups have significant USPIO-labeled macrophage infiltration. USPIO-labeled macrophage infiltration is greatly reduced in the clodronate-liposome-treated allogaft hearts, although there is still low level observed. All the native hearts (Figure 3B, H, D, J, F, L) from the same treated animals have very little USPIO-labeled accumulation, indicating that the macrophage infiltration into rejecting allograft hearts is specific and selective.

Immunohistochemical staining of the allograft hearts (Figure 4) confirms the cellular MRI finding. Both untreated (Figure 4A) and PBS-liposome controls (Figure 4B) exhibit significantly more ED1+ macrophage infiltration on POD 7 than clodronate-liposome-treated heart (Figure 4C).

Reducing macrophage infiltration resulting in preserved tissue integrity

The graft tissue integrity is evaluated with H&E tissue staining (Figure 5). On POD 7, as rejection progresses to a more severe stage, untreated allografts (Figure 5B) loose myocardium integrity with visible cellular infiltration. No untreated allografts can sustain past POD 8. On the contrary, the clodronate-liposome-treated allografts show a marked improvement in tissue integrity on POD 7 (Figure 5C), similar to the isografts (Figure 5A) with no rejection. By POD 9 (Figure 5D), the clodronate-liposome-treated allografts start to show signs of acute rejection, exhibiting increased infiltration of mononuclear cells and tissue injury.

Reducing macrophage infiltration resulting in preserved cardiac function

To assess whether reducing only one cell type, macrophages, without affecting other immune cells, is sufficient to attenuate acute allograft rejection, we have examined the functional consequences of clodronate-liposome treatment. We have shown that strain values derived from myocardial-tagged MRI can best differentiate regional wall-motion changes resulting from acute allograft rejection[6]. Figure 6 shows Ecc maps derived from the tagged MRI of an untreated (Figure 6A), a PBS-liposome-treated (Figure 6B), and a clodronate-liposome-treated (Figure 6C) allograft heart over time. With no treatment, allograft hearts undergo normal progression of acute rejection over time (Figure 6A and Figure 6D, blue circles), exhibiting a sharp decrease in the LV wall motion. The clodronate-liposome-treated allograft hearts (Figure 6C and Figure 6D, red squares) exhibit improved wall motion from POD 5 to POD 6, myocardial areas with medium-to-high strain values increases, and the subsequent functional loss from POD 7 to 9 is significantly less. The PBS-liposome-treated allograft heart (Figure 6B and Figure 6D, green triangles), although showing slight improvement in function early on, the cardiac function also degrades sharply after POD 6.

Figure 7 shows mean circumferential strain (Figure 7A, Ecc) and radial strain (Figure 7B, Err) values of all allografts over time as the rejection progresses. Untreated allografts display a sharp decrease in strain over time, as acute rejection progresses. Conversely, clodronate-liposome-treated allograft hearts exhibit improved strain and cardiac function in the early phase, and then decrease in functions later in time. Vast majority of untreated allograft hearts loose function with no detectable ECG on POD 7; and none can sustain past POD 8. PBS-liposome-treated allografts also undergo functional deterioration over time, but the progress of the dysfunction follows a slower time course, compared to that of the untreated group. On POD 7, when most untreated allografts are not functional, the PBS-liposome-treated allografts still preserve cardiac function that is comparable to the clodronate-liposome-treated allografts. However, PBS-liposome-treated allograft hearts continue to lose contractility, and by POD 9, they have become not functional, with no meaningful strain values detected. On the contrary, clodronate-liposome-treated allograft hearts have preserved wall motion with little or no decline up to POD 7, and still maintain more than 80 % of the strain values on POD 9. There was no statistically significant difference in the strains for the clodronate-liposome-treated hearts between PODs 7 an 9 (Ecc p=0.6689; Err p=0.8533); but both circumferential and radial strains showed significant differences between the clodronate-liposome-treated and PBS-liposome-treated hearts (Ecc p=0.0289; Err p=0.0009) on POD 9.

Our results demonstrate that clodronate-liposome treatment can preserve cardiac tissue integrity and preserve cardiac function in acute allograft rejection. This indicates that clodronate-liposome treatment significantly alters the progression of acute rejection in allograft hearts, and that macrophages play a significant role in the progression of acute rejection.

Discussion

Following transplantation, patients must endure a life-long regiment of immunosupression therapy. Despite the medical advancement, allograft rejection remains a threat to the long-term survival and new therapeutic methods and monitoring strategies to improve and personalize treatment are much needed. The current immunosupression therapy is mainly focused on blocking T-lymphocytes, or general broad-band immune-suppression. In this study, we have looked at the specific effects of macrophages on the cardiac allograft rejection by selectively depleting macrophages with intravenous injections of clodronate-encapsulated liposomes [7, 8]. It has been reported that this strategy is effective for delaying rejection in rat corneal allografts [18, 19], pig pancreas xenografts [20, 21], liver transplantation [22], and rat renal allografts [23], however, its use in a cardiac transplantation had not yet been studied. Our approach to simultaneously monitor cellular infiltration and cardiac function by MRI provides a good platform to non-invasively monitor the immune cell infiltration and the functional consequences longitudinally over time.

We have previously demonstrated that standard cardiac MRI protocols, such as cine imaging and the the global systolic functional parameters derived from cine, ejection fraction (EF) or stroke volume (SV), are not sensitive in discriminating rejecting allograft hearts from non-rejecting isografts, especially in the earlier rejection stages [6]. We have shown that myocardial strains derived from tagging MRI are more sensitive and accurate parameters that can better quantify various rejection grades in acute allograft rejection [6]. Since the focus of this study is to investigate the effects of clodronate-liposomes on cardiac function in allograft rejection, we have used the cardiac MRI parameters, strains derived from tagging MRI, that we have established best for assessing allograft rejection.

In the rat transplantation model used in this study, we have previously demonstrated that the BN-to-BN isograft hearts (with no rejection) exhibited wall motion and strain values comparable to those of the native hearts, although SV was somewhat less.[6] The graft hearts in this model preserve intact pulmonary circulation and all 4 heart chambers exhibit wall motion and strains that are close to native hearts[6], and show similar pathological features as human transplanted hearts determined histopathologically according to the updated International Society for Heart and Lung Transplantation (ISHLT) criteria for human patients[24]. In addition, since the recipient animal still has the intact native heart to support life, the complete rejection process can be studied with minimal systemic deterioration to the host. In our model, the untreated rats have a sharp decline in allograft cardiac function between POD 5 and 7. Most of the untreated allograft hearts lose all function by POD 7, and none can survive to POD 8. With this heterotopic transplantation model, however, the host heart maintains normal circulation and physiology over the entire rejection process because the native heart supports life. Our findings show that the depletion of macrophages over the course of the experiment results in markedly improved allograft function and survival. In the transplant recipients receiving clodronate-liposomes on days 1, 3, 6, and 8 post-transplantation, the allograft hearts survived to POD 9, with preserved myocardial tissue integrity and cardiac function. There was no sign of functional deterioration in allograft hearts on PODs 5–7 with the clodronate-liposome treatment, and in some cases, the cardiac function improved from POD 5 to 7. From PODs 7–9, when all allografts from the control groups have failed, the clodronate-liposome-treated allografts still maintained over 80%

normal wall motion. Strain values for the clodronate-liposome-treated allograft hearts showed no statistically significant differences from POD 5 to 9. We chose POD 9 as the endpoint of this study, because by POD 9, PBS-treated-allograft hearts have lost myocardial function, exhibiting strains similar to those of no-treatment group on POD7, when severe allograft rejection occurred. Additional studies will be needed to determine the longer term outcome of macrophage depletion. It is important to note that the rats seemed to tolerate the repeated clodronate-liposome treatments well, and no adverse effects overall physiology were noted.

Although clodronate-liposomes were developed to deplete mature macrophages, Sunderkotter et al. [25] have reported that all circulating monocytes were depleted as well. Our flow cytometry (Figure 1) and cellular MRI results (Figure 2, 3) show that ED1+ monocytes and macrophages decrease significantly upon the clodornate-liposome treatment in both circulation and rejecting allograft hearts. In our present study, we began the clodronate-liposome treatment one day post-transplantation. By this time, there were macrophages present in the graft tissue. In addition to donor resident macrophages within the graft, a high influx of recipient monocytes/macrophages was known to enter graft heart immediately following transplantation in response to the surgical trauma and ischemic reperfusion injury. The subsequent macrophage population was then affected by the recruitment from circulation, exiting, local proliferation, and/or cell death. This is consistent with recent findings that the tissue macrophages have fast turnover kinetics [4] and monocytes/macrophages are constantly recruited. Other phagocytic cells, such as dendritic cells, could potentially be affected by clodronate-liposome treatment as well; however, they are rare in the circulating hematopoietic mixture, but are mobilized into circulation from tissues and organs in response to pathological conditions.

About two-thirds of the clodronate-liposome treated animals did experience an unusual phenomenon, in that a solid mass had developed inside the left ventricle of the transplanted heart, but not seen in the native hearts of the same animals. This mass did appear to physically hinder ventricular wall motion and affect strain measurements, in some cases; however, these hearts still exhibited better stain values than the controls and were not excluded from analysis. The size of the deposit varied greatly, and the mass was not seen in PBS-liposome-controls, or any native hearts. The source of the mass is not known, but preliminary NMR spectroscopy results suggest a lipid component similar to the liposome vehicle used (results not shown). One possibility is that the mass might be an accumulation of macrophage and/or liposome debris. Frantz and associates reported in an experimental myocardial infarction model that the clodronate-liposome treatment resulted in thrombus formation in LV [26]. Figure 8 shows the H&E staining of the mass found in the transplanted hearts treated with clodronate-liposomes. In our model, the mass does not seem to be thrombus; rather, it appears to be layers of lipid. The lack of deposits in PBS-liposome-treated allografts is consistent with the observation that there is no massive macrophage death, and functional macrophages can clear debris from circulation. A different treatment regimen may mitigate the accumulation of the material in the LV cavity, but this will require further study. Before exploring potential clinical applications, further optimization of the clodronate-liposome dosing protocol is necessary to better understand and minimize any potential adverse effects such as the intra-ventricular mass observed in this study.

It is interesting to note that the PBS-liposome-treated group appears to display a slower decline in cardiac function in the earlier phases, compared to the allograft hearts receiving no treatment, but none of the PBS-liposome treated allografts can maintain function beyond POD 8, as observed with the clodronate-liposome treatment. The fact that the PBS-liposome-treated allografts show improvement indicates that liposomes, or certain lipid components of the liposomes, may have beneficial effects for the graft hearts. Alternatively,

although PBS-liposomes do not deplete macrophages as clodronate-liposomes do, PBS-liposomes may temporarily block certain macrophage functions [7], or may affect other systemic or regional immune responses. Further studies are needed to investigate the mechanism of this interesting observation. Nevertheless, PBS-liposomes do not preserve allograft hearts against allograft rejection on POD 9 as clodronate-liposomes do.

Monocytes and macrophages are centrally involved in multitude of disorders that have high impact, such as cardiovascular diseases, cancer, trauma, and autoimmune diseases [27]. Monocytes and macrophages are emerging therapeutic targets in cardiovascular disease; however, clinical tools to assess their presence in tissue are scarce[4, 28]. Superparamagnetic iron-oxide nanoparticles (SPIO) and ultra-small superparamagnetic iron-oxide nanoparticles (USPIO) can be used to monitor cell movement by *in-vivo* MRI as a function of time[5, 6]. Recently, there are several human studies utilizing iron-oxide particles to image myocardial inflammation in patients with acute myocardial infarction [29, 30]. Clinical translation of cellular MRI to track myocardial inflammation is feasible.

The differences in the affinity of different types of monocytes/macrophages to different magnetic nanoparticles and contrast agents have been studied recently in *ex-vivo* cell culture systems[31, 32]. In our study, we did not discriminate different sub-types of macrophages. Further studies are needed to discern if different phenotypes of macrophages possess different *in-vivo* labeling efficiency.

In conclusion, reducing macrophage infiltration in allograft hearts is shown to preserve cardiac tissue, prolong the graft survival, and protect dysfunction as a result of acute cardiac rejection. Our results suggest that macrophages in the graft is an essential key trigger for propagating the acute allograft rejection cascade, and may serve as an *in-situ* biomarker for acute cardiac rejection. Selective elimination of circulating monocytes and macrophages with appropriate timing may be an effective strategy to reduce harmful immune response following transplantation. Additionally, new strategies may be developed to target certain macrophage activities, or inhibiting certain macrophage-associated-cytokines, without completely eliminating them from the body.

Supplementary Material

Refer to Web version on PubMed Central for supplementary material.

Acknowledgments

Sources of Funding

This study is supported by grants from the National Institutes of Health (P41EB-001977, R01HL-081349, UL1 RR024153 and UL1TR000005), and the Health Research Formula Funds of the Commonwealth University Research Enhancement Section of the Tobacco Settlement Act 47 (Grant ME-02-168). LL was supported by an American Heart Association Great Rivers Affiliate Postdoctoral Fellowship (10POST3010016).

ABBREVIATIONS

MRI	magnetic resonance imaging
MRM	magnetic resonance microscopy
USPIO	ultra-small superparamatic-iron-oxide
PBS	phosphate-buffered saline
ECG	electrocardiogram

POD	post-operational day
LV	left ventricle
TE	echo time
TR	repetition time
FOV	field of view
Ecc	circumferential strain
Err	radial strain
Tx Ht	transplanted graft heart
Tx Lung	transplanted graft lung

References

1. Mannon RB. Macrophages: Contributors to allograft dysfunction, repair, or innocent bystanders? Curr Opin Organ Transplant. 2012; 17:20–25. [PubMed: 22157320]
2. Fleming BD, Mosser DM. Regulatory macrophages: Setting the threshold for therapy. Eur J Immunol. 2011; 41:2498–2502. [PubMed: 21952805]
3. Mosser DM, Edwards JP. Exploring the full spectrum of macrophage activation. Nat Rev Immunol. 2008; 8:958–969. [PubMed: 19029990]
4. Leuschner F, Rauch PJ, Ueno T, Gorbatov R, Marinelli B, Lee WW, Dutta P, Wei Y, Robbins C, Iwamoto Y, Sena B, Chudnovskiy A, Panizzi P, Keliher E, Higgins JM, Libby P, Moskowitz MA, Pittet MJ, Swirski FK, Weissleder R, Nahrendorf M. Rapid monocyte kinetics in acute myocardial infarction are sustained by extramedullary monocytopoiesis. J Exp Med. 2012; 209:123–137. [PubMed: 22213805]
5. Wu YL, Ye Q, Foley LM, Hitchens TK, Sato K, Williams JB, Ho C. In situ labeling of immune cells with iron oxide particles: An approach to detect organ rejection by cellular mri. Proc Natl Acad Sci U S A. 2006; 103:1852–1857. [PubMed: 16443687]
6. Wu YL, Ye Q, Sato K, Foley LM, Hitchens TK, Ho C. Noninvasive evaluation of cardiac allograft rejection by cellular and functional cardiac magnetic resonance. JACC Cardiovasc Imaging. 2009; 2:731–741. [PubMed: 19520344]
7. Van Rooijen N, Sanders A. Liposome mediated depletion of macrophages: Mechanism of action, preparation of liposomes and applications. J Immunol Methods. 1994; 174:83–93. [PubMed: 8083541]
8. van Rooijen N, Sanders A, van den Berg TK. Apoptosis of macrophages induced by liposome-mediated intracellular delivery of clodronate and propamidine. J Immunol Methods. 1996; 193:93–99. [PubMed: 8690935]
9. Dodd SJ, Williams M, Suhan JP, Williams DS, Koretsky AP, Ho C. Detection of single mammalian cells by high-resolution magnetic resonance imaging. Biophys J. 1999; 76 (1 Pt1):103–109. [PubMed: 9876127]
10. Varallyay P, Nesbit G, Muldoon LL, Nixon RR, Delashaw J, Cohen JI, Petrillo A, Rink D, Neuwelt EA. Comparison of two superparamagnetic viral-sized iron oxide particles ferumoxides and ferumoxtran-10 with a gadolinium chelate in imaging intracranial tumors. AJNR Am J Neuroradiol. 2002; 23:510–519. [PubMed: 11950637]
11. Axel L, Dougherty L. Heart wall motion: Improved method of spatial modulation of magnetization for mr imaging. Radiology. 1989; 172:349–350. [PubMed: 2748813]
12. Axel L, Dougherty L. Mr imaging of motion with spatial modulation of magnetization. Radiology. 1989; 171:841–845. [PubMed: 2717762]
13. Castillo E, Osman NF, Rosen BD, El-Shehaby I, Pan L, Jerosch-Herold M, Lai S, Bluemke DA, Lima JA. Quantitative assessment of regional myocardial function with mr-tagging in a multi-

center study: Interobserver and intraobserver agreement of fast strain analysis with harmonic phase (harp) mri. J Cardiovasc Magn Reson. 2005; 7:783–791. [PubMed: 16358393]

14. Osman NF, McVeigh ER, Prince JL. Imaging heart motion using harmonic phase mri. IEEE Trans Med Imaging. 2000; 19:186–202. [PubMed: 10875703]
15. Otsu N. A threshold selection method from gray-level histograms. Automatica. 1975; 11:23–27.
16. Tan CD, Baldwin WM 3rd, Rodriguez ER. Update on cardiac transplantation pathology. Arch Pathol Lab Med. 2007; 131:1169–1191. [PubMed: 17683180]
17. Dunn OJ. Multiple comparisons using rank sums. Technometrics. 1964; 6:241–252.
18. Torres PF, Slegers TP, Peek R, van Rooijen N, van der Gaag R, Kijlstra A, de Vos AF. Changes in cytokine mrna levels in experimental corneal allografts after local clodronate-liposome treatment. Invest Ophthalmol Vis Sci. 1999; 40:3194–3201. [PubMed: 10586942]
19. Slegers TP, van Rooijen N, van Rij G, van der Gaag R. Delayed graft rejection in pre-vascularised corneas after subconjunctival injection of clodronate liposomes. Curr Eye Res. 2000; 20:322–324. [PubMed: 10806446]
20. Fox A, Koulmanda M, Mandel TE, van Rooijen N, Harrison LC. Evidence that macrophages are required for t-cell infiltration and rejection of fetal pig pancreas xenografts in nonobese diabetic mice. Transplantation. 1998; 66:1407–1416. [PubMed: 9869080]
21. Wu G, Korsgren O, Zhang J, Song Z, van Rooijen N, Tibell A. Pig islet xenograft rejection is markedly delayed in macrophage-depleted mice: A study in streptozotocin diabetic animals. Xenotransplantation. 2000; 7:214–220. [PubMed: 11021667]
22. Akamatsu Y, Ohkohchi N, Doi H, Satomi S. Effect of elimination of donor kupffer cells and/or recipient macrophages on acute rejection in liver transplantation. Hepatogastroenterology. 2003; 50:1105–1110. [PubMed: 12845991]
23. Jose MD, Ikezumi Y, van Rooijen N, Atkins RC, Chadban SJ. Macrophages act as effectors of tissue damage in acute renal allograft rejection. Transplantation. 2003; 76:1015–1022. [PubMed: 14557746]
24. Stewart S, Winters GL, Fishbein MC, Tazelaar HD, Kobashigawa J, Abrams J, Andersen CB, Angelini A, Berry GJ, Burke MM, Demetris AJ, Hammond E, Itescu S, Marboe CC, McManus B, Reed EF, Reinsmoen NL, Rodriguez ER, Rose AG, Rose M, Suciu-Focia N, Zeevi A, Billingham ME. Revision of the 1990 working formulation for the standardization of nomenclature in the diagnosis of heart rejection. J Heart Lung Transplant. 2005; 24:1710–1720. [PubMed: 16297770]
25. Sunderkotter C, Nikolic T, Dillon MJ, Van Rooijen N, Stehling M, Drevets DA, Leenen PJ. Subpopulations of mouse blood monocytes differ in maturation stage and inflammatory response. J Immunol. 2004; 172:4410–4417. [PubMed: 15034056]
26. Frantz S, Hofmann U, Fraccarollo D, Schafer A, Kranepuhl S, Hagedorn I, Nieswandt B, Nahrendorf M, Wagner H, Bayer B, Pachel C, Schon MP, Kneitz S, Bobinger T, Weidemann F, Ertl G, Bauersachs J. Monocytes/macrophages prevent healing defects and left ventricular thrombus formation after myocardial infarction. FASEB J. 2013; 27:871–881. [PubMed: 23159933]
27. Nahrendorf M, Swirski FK. Monocyte and macrophage heterogeneity in the heart. Circ Res. 2013; 112:1624–1633. [PubMed: 23743228]
28. Lee WW, Marinelli B, van der Laan AM, Sena BF, Gorbatov R, Leuschner F, Dutta P, Iwamoto Y, Ueno T, Begieneman MP, Niessen HW, Piek JJ, Vinegoni C, Pittet MJ, Swirski FK, Tawakol A, Di Carli M, Weissleder R, Nahrendorf M. Pet/mri of inflammation in myocardial infarction. J Am Coll Cardiol. 2012; 59:153–163. [PubMed: 22222080]
29. Alam SR, Shah AS, Richards J, Lang NN, Barnes G, Joshi N, MacGillivray T, McKillop G, Mirsadraee S, Payne J, Fox KA, Henriksen P, Newby DE, Semple SI. Ultrasmall superparamagnetic particles of iron oxide in patients with acute myocardial infarction: Early clinical experience. Circ Cardiovasc Imaging. 2012; 5:559–565. [PubMed: 22875883]
30. Richards JM, Shaw CA, Lang NN, Williams MC, Semple SI, MacGillivray TJ, Gray C, Crawford JH, Alam SR, Atkinson AP, Forrest EK, Bienek C, Mills NL, Burdess A, Dhaliwal K, Simpson AJ, Wallace WA, Hill AT, Roddie PH, McKillop G, Connolly TA, Feuerstein GZ, Barclay GR, Turner ML, Newby DE. In vivo mononuclear cell tracking using superparamagnetic particles of

iron oxide: Feasibility and safety in humans. Circ Cardiovasc Imaging. 2012; 5:509–517. [PubMed: 22787016]

31. Settles M, Etzrodt M, Kosanke K, Schiemann M, Zimmermann A, Meier R, Braren R, Huber A, Rummeny EJ, Weissleder R, Swirski FK, Wildgruber M. Different capacity of monocyte subsets to phagocytose iron-oxide nanoparticles. PLoS One. 2011; 6:e25197. [PubMed: 21984904]
32. Satomi T, Ogawa M, Mori I, Ishino S, Kubo K, Magata Y, Nishimoto T. Comparison of contrast agents for atherosclerosis imaging using cultured macrophages: Fdg versus ultrasmall superparamagnetic iron oxide. J Nucl Med. 2013; 54:999–1004. [PubMed: 23670898]

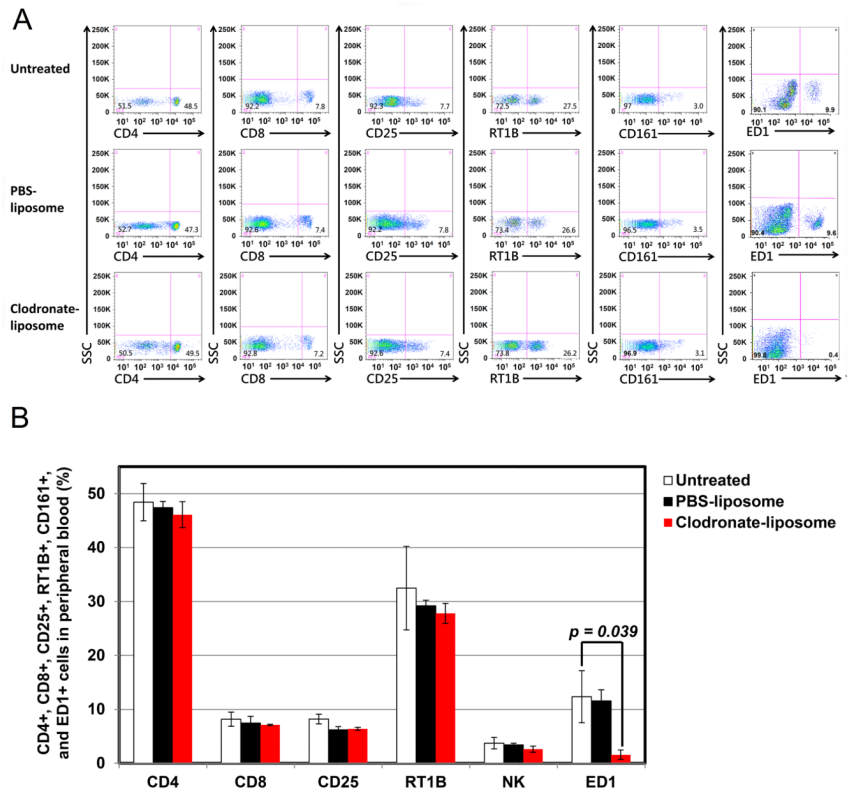

Figure 1.

Clodronate-liposome treatment selectively reduces macrophages in circulation, but not affecting other lymphocytes: (A) Flow cytometry analysis of blood leukocytes of untreated (top panel), PBS-liposome (middle panel), and clodronate-liposome (bottom panel) treated transplantation recipients (on POD 7) demonstrates that there is a depletion of ED+ cells, but no significant alternation in other leukocytes, including CD4+, CD8+, CD25+, class II, and NK cells in the peripheral blood, upon treatment with clodronate-liposome; and (B) Numerical presentation of the cytometric analysis from (A). Significant differences in ED1+ cells are found between the groups on POD7. For ED1+, post-hoc comparisons revealed significantly smaller ED1+ cells for the clodronate-liposome group when compared to untreated and PBS-liposome groups.

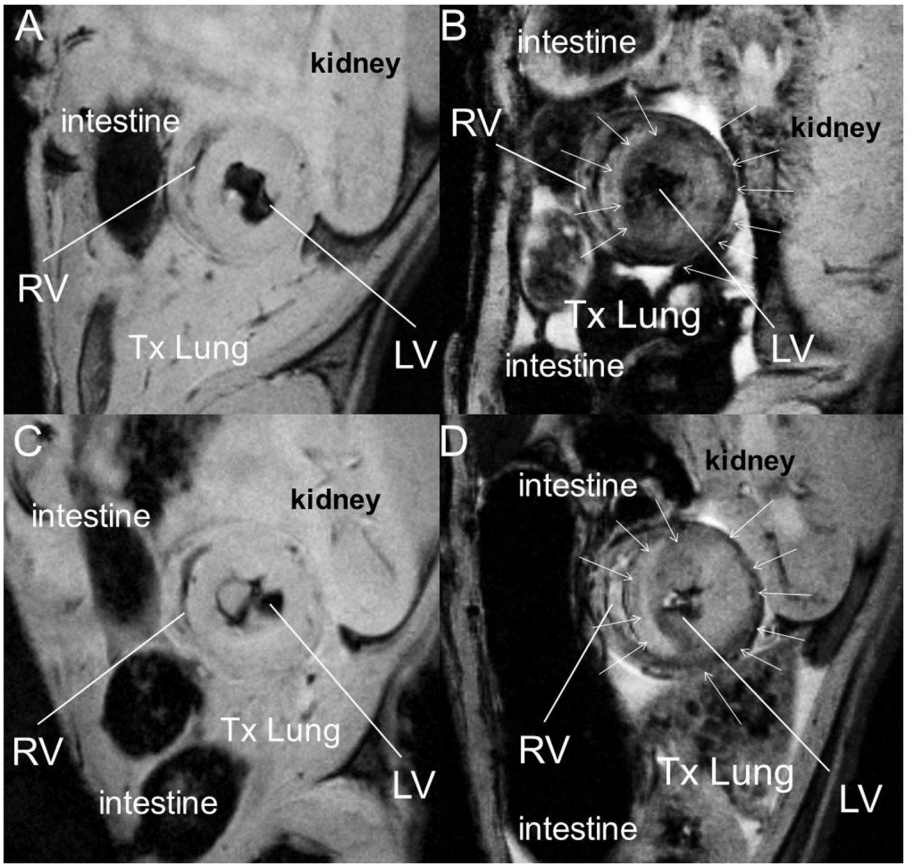

Figure 2.

Clodronate-liposome treatment reduces macrophages infiltration in the rejecting allograft hearts, evaluated by *in-vivo* T_2^*-weighted cellular MRI with *in-vivo* USPIO labeling: (A) Representative pre-contrast image of a transplanted heart; (B) No-treatment regular rejecting allograft heart; (C) clodronate-treated rejection allograft heart; and (D) PBS-liposome-treated allograft heart. Hypointensity, resulting from USPIO-labeled macrophages infiltrated in the rejecting allograft hearts, can be seen in the no-treatment control (B) and PBS-liposome treated alllograft (D), but not in the clodronate-treated allograft (C). T_2^*-weighted MR images were acquired at 7-Tesla, with 156-μm in-plane resolution. Arrowheads point to areas with USPIO-labeled macrophage infiltration.

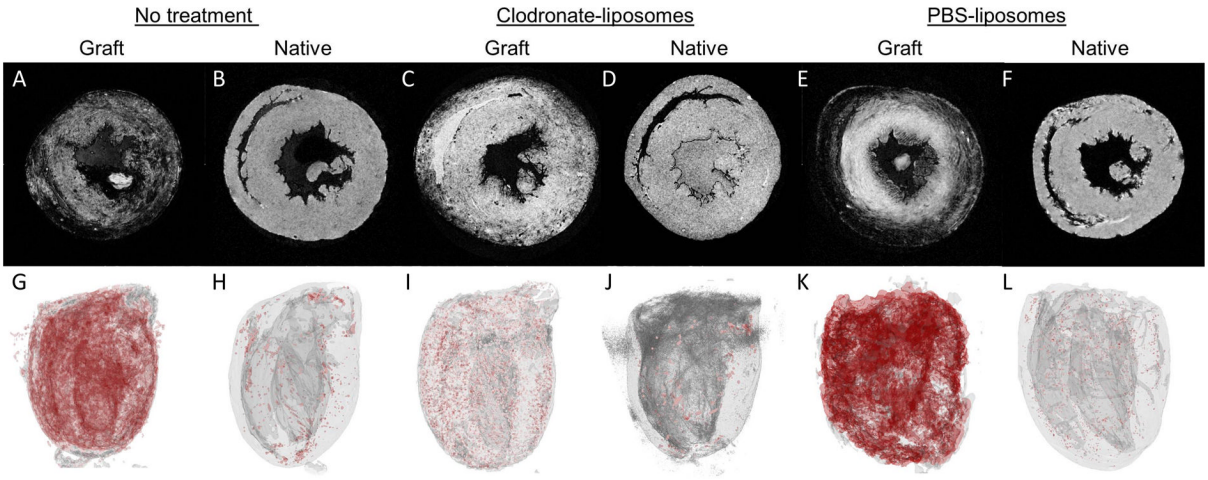

Figure 3.

Clodronate-liposome treatment reduces macrophages infiltration in the rejecting allograft hearts, evaluated by *ex-vivo* T_2^*-weighted 3D MR Microscopy (MRM). (Upper panels, A–F): One 2D image from the 3D MRM image stacks; (lower panels: G – L); 3D volume rendering, with hypointensity showing in red color, of a no-treatment allograft heart (A, G); clodronate-liposome-treated allograft heart (C, I); and PBS-liposome-treated allograft heart (E, K); as well as native hearts from the same no-treatment animal (B, H), the clodronate-liposome-treated animal (D, J), and the PBS-liposome-treated animal (F, L). T_2^*-weighted MRM was acquired at 11.7-Tesla with 46 to 49-μm isotropic resolution.

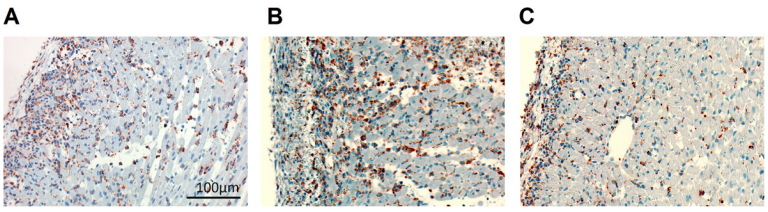

Figure 4.

Clodronate-liposome treatment reduces macrophages infiltration in the rejecting allograft hearts, evaluated by immunohistochemical staining of anti-rat $ED1^{+}$ in allograft hearts on POD 7: (A) untreated allograft; (B) PBS-liposome-treated allograft; and (C) clodronate-liposome treated allograft. ED1+ macrophages are in brown color.

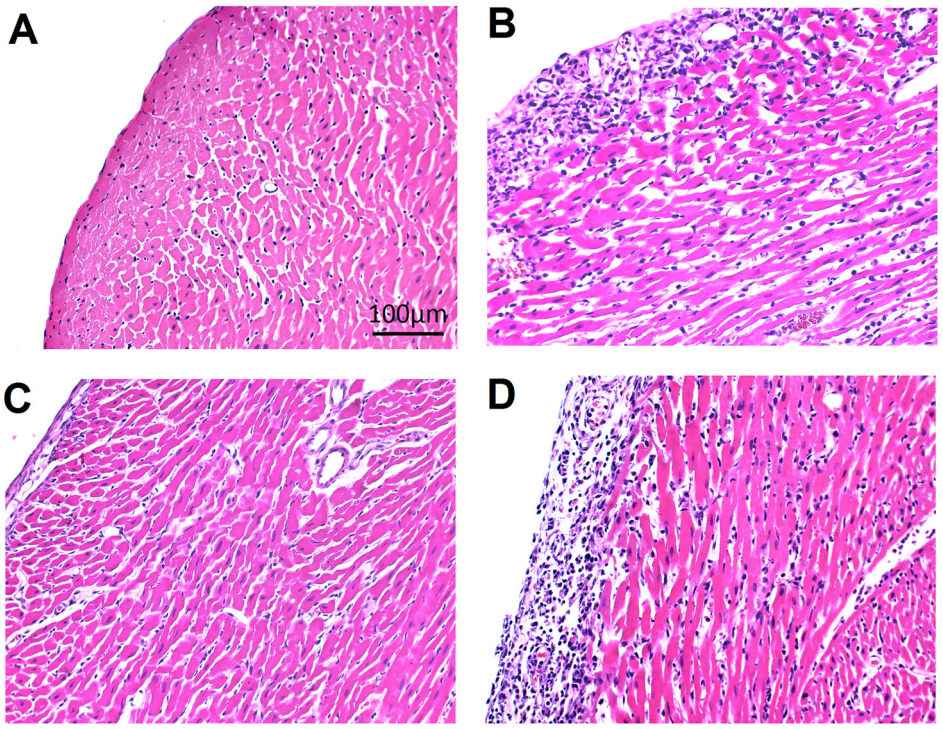

Figure 5.
Clodronate-liposome treatments preserve tissue integrity, evaluate by H&E tissue staining of (A) an isograft and (B–D) three allografts hearts. Untreated isograft and allograft hearts on POD 7 are shown in (A) and (B); (C) a clodronate-liposome treated allograft on POD 7, which reveals decreased damage to the tissue of the graft compared to the untreated allograft on the same day (B); (D) a clodronate-liposome treated allograft on POD 9.

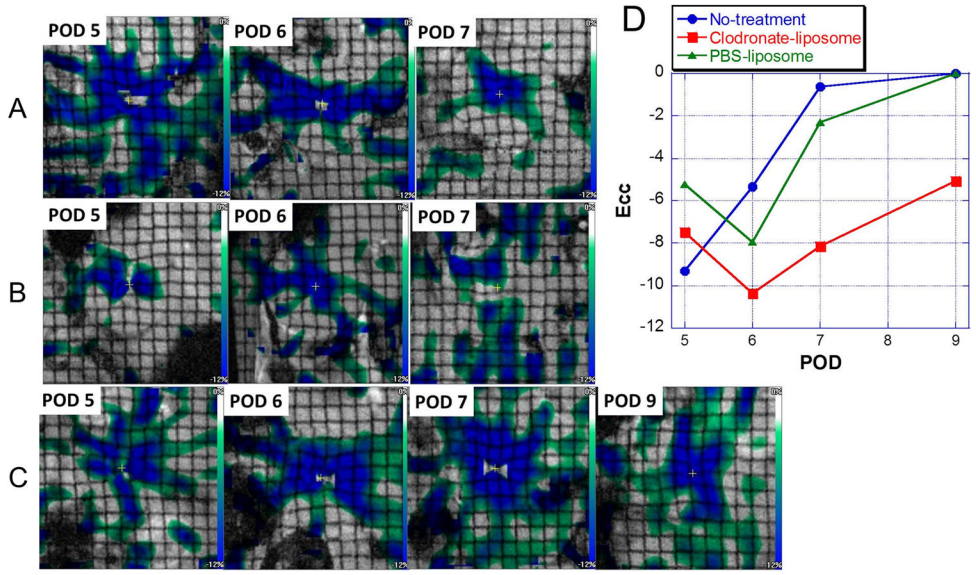

Figure 6.

Circumferential strain (Ecc) maps of the same allograft hearts over time, derived from tagging MRI for (A) a no-treatment allograft heart; (B) a PBS-liposome treated allograft heart; and (C) a clodronate-liposome treated allograft heart. (D) Mean Ecc values across the LV wall of the individual hearts shown in A, B, and C, on each POD. Blue circles: the no-treatment control allograft heart; red squares: the clodronate-liposome treated allograft heart; and green triangles: the PBS-liposome treated allograft heart.

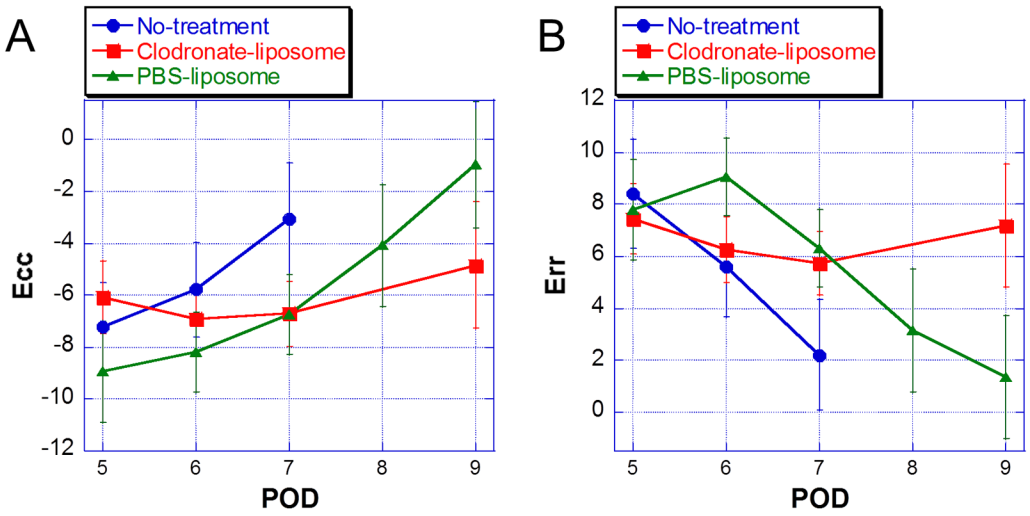

Figure 7.

(A) Estimated Ecc values are expected means from the linear mixed-effects model. Error bars indicate 95% confidence intervals. Linear mixed-effects model analysis shows a significant interaction between treatment group and time [$F(5,70)=3.49$, $p=0.0071$] for Ecc. Results show that Ecc is increasing over time for PBS-liposome and No-Treatment groups, whereas Ecc for the clodronate-liposome group is not. Further examination has revealed differences between treatment groups on POD 7 and POD 9. On POD 7, PBS-liposome and clodronate-liposome are approximately 3.70 below the no-treatment group in terms of the mean of Ecc (PBS-liposome vs no-treatment, [$t(82)$, $p=0.0066$]; clodronate vs no-treatment, [$t(82)$, $p=0.0043$]. In addition, statistically significant difference between PBS-liposome and clodronate-liposome groups are found on POD 9 [($t(81)$, $p=0.0285$], clodronate-liposome group is 3.87 below the PBS-liposome group in terms of mean Ecc. Adjusted p-values are shown. (B) Estimated Err values are expected means from the linear mixed-effects model. Error bars indicate 95% confidence intervals. Linear mixed-effects model analysis shows a significant interaction between time and treatment group [$F(5,66)=5.81$, $p=0.0002$]. Results show that all groups have similar Err means on POD 5. Then, Err is generally decreasing over time for both PBS-liposome and no-Treatment groups, whereas Err for the clodronate-liposome group is not. No statistically significant differences among groups were found on POD 5. Results show significant differences at POD 6 between PBS-liposome and clodronate-liposome groups [$t(82)=-2.86$, $p=0.0054$], and between PBS-liposome and no-treatment groups [$t(82)=-2.83$, $p=0.0059$]. In addition, on POD 7, significant differences are found between no-treatment and PBS-liposome groups [$t(82)=-3.13$, $p=0.0024$] and between no-treatment and clodronate-liposome groups [$t(82)=-2.87$, $p=0.0052$] on POD 7. Significant difference between PBS-liposome and clodronate-liposome groups [$t(83)=3.47$, $p=0.0008$] is also found on POD 9. Adjusted p-values are shown: blue circles, the no-treatment control allograft hearts; red squares, the clodronate-liposome treated allograft hearts; and green triangles, the PBS-liposome treated allograft hearts. Lines are drawn between data points for visualization purpose.

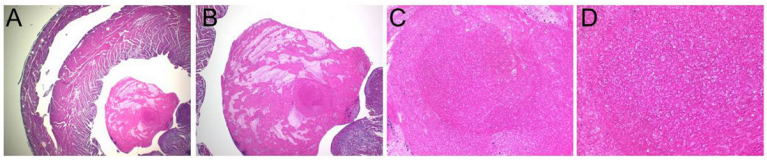

Figure 8.
A representative of H & E staining of the mass found in the LV: (A) magnification 20 X; (B) magnification 40X; (C) magnification 200X; and (D) magnification 400X.